



ELSEVIER

Available online at [www.sciencedirect.com](http://www.sciencedirect.com)

SCIENCE @ DIRECT®

Journal of Non-Crystalline Solids xxx (2003) xxx–xxx

JOURNAL OF  
NON-CRYSTALLINE SOLIDS[www.elsevier.com/locate/jnoncrysol](http://www.elsevier.com/locate/jnoncrysol)

# Anomalous temperature dependence of sub-critical crack growth in silica glass

T.I. Suratwala <sup>\*</sup>, R.A. Steele*Lawrence Livermore National Laboratory, P.O. Box 808, Livermore, CA 94551, USA*

Received 16 January 2002; received in revised form 10 July 2002

## Abstract

The effects of temperature, water vapor, and stress on the rate of sub-critical crack growth (SCG) in fused silica are reported. The crack velocity was measured using the double-cleavage-drilled compression method. In contrast to other inorganic oxide glasses, crack growth velocities (in region I) were found to decrease with increase in temperature. Hence a small temperature rise has the apparent effect of improving the mechanical strength of a stressed-glass part. Despite the anomalous temperature dependence, SCG in fused silica is still likely governed by the established water-enhanced stress–corrosion mechanism; another competing phenomenon is proposed to cause the observed temperature dependence. Measured crack velocities are described using an empirical model (for region I) and a mass-transport model limited by Knudsen diffusion (for region II).

© 2003 Published by Elsevier Science B.V.

## 1. Introduction

Vitreous or fused silica (i.e. SiO<sub>2</sub> glass) is a technologically important material because of its excellent optical qualities, low thermal expansion, and resistance to both high temperature and chemical corrosion. In many use applications, fused silica parts are often subjected to a range of mechanical stresses. Under such conditions, small pre-existing flaws in the glass can grow at stresses below the critical stress needed to cause failure. This type of crack growth, often called sub-critical crack growth (SCG), stress–corrosion cracking, or

slow crack growth, occurs in many materials such as metals, ceramics, polymers and glasses. A slowly growing crack on an automobile windshield is a common example of SCG. The velocity of the fracture can vary by orders of magnitude from less than 0.1 μm/min to a fraction of the speed of sound (~10<sup>9</sup> μm/min); therefore the failure time for a component can also vary by orders of magnitude.

Atomistically, the fracture of SiO<sub>2</sub> glass involves the cleavage of oxide bonds as the crack front propagates. Because of the strong covalent bonding and the unique network of SiO<sub>4</sub> tetrahedra, SiO<sub>2</sub> glass is intrinsically one of the strongest materials. However, its strength is dramatically reduced by the chemical attack by water [1]. In the case of silicate glasses under stress, water lowers the energy required to cleave a siloxane bond:

<sup>\*</sup> Corresponding author. Tel.: +1-925 422 1884; fax: +1-925 423 0792.

E-mail address: [suratwala1@llnl.gov](mailto:suratwala1@llnl.gov) (T.I. Suratwala).

$\text{H}_2\text{O} + \text{Si-O-Si} \rightarrow 2(\text{Si-OH})$ . An increase in temperature enhances this stress corrosion reaction rate, and, therefore, SCG should increase with temperature.

Previous studies of SCG in fused silica have been performed in various liquids (water, alcohols, etc.), vacuum, and air at various humidities [2–7]. However, little has been reported on the effect of temperature on fused silica SCG in air at a constant water vapor pressure.

In this study, SCG velocities in fused silica are measured in air at various temperatures, water vapor pressures, and stresses using the double-cleavage-drilled compression (DCDC) method. Instead of increasing with temperature (in region I), as observed in most glasses, crack velocities in fused silica are found to decrease with tempera-

ture. The practical implication is that an increase in temperature can potentially increase the resistance of fused silica glass to further crack growth. Potential mechanisms for the anomalous temperature dependence are qualitatively described, and an empirical model is used to describe the data. Then, the region II crack velocity behavior of fused silica is compared to the behavior observed in other glasses, and the data is described using a Knudsen diffusion mass-transport model.

## 2. Experimental

The SCG velocities of fused silica glass (Corning 7980, ~1000 ppm by weight OH) were measured using the DCDC technique [8–10]. A

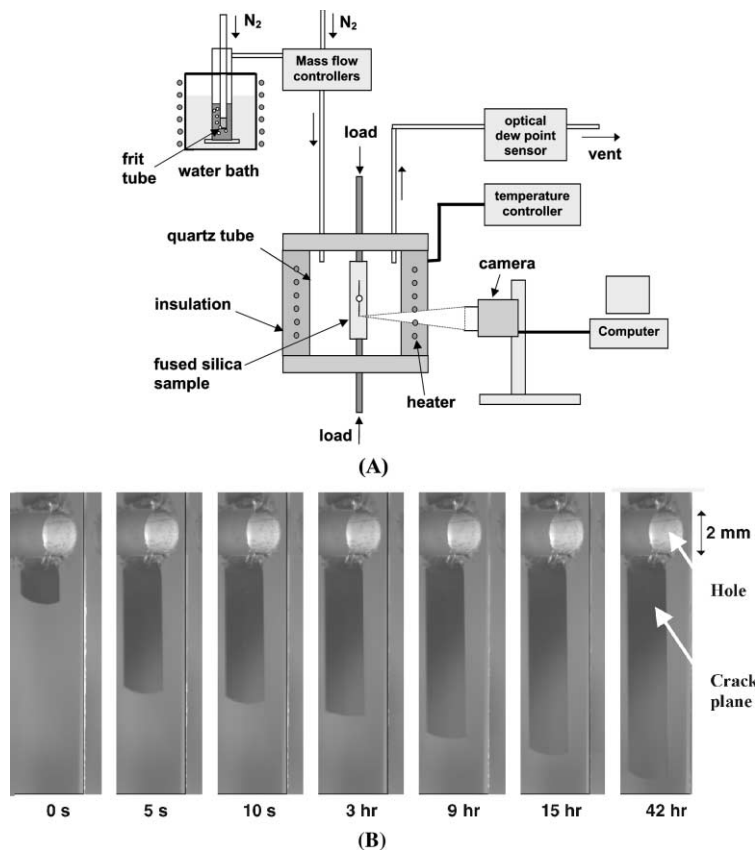


Fig. 1. (A) Schematic of the experimental setup used to measure SCG velocities using the DCDC method. (B) Images of a propagating crack ( $T = 25^\circ\text{C}$ ,  $P_{\text{H}_2\text{O}} = 0.3\text{ Pa}$ , applied stress = 88 MPa) in fused silica at various times viewed  $\sim 45^\circ$  from the hole-drill axis. Dark regions in the images represent the fracture plane that initiated from 2 mm hole.

schematic of the experimental setup is shown in Fig. 1(A). During the measurement, cut and polished rectangular glass ( $75 \times 6.5 \times 7.5 \text{ mm}^3$ ) samples with a 2 mm diameter drilled hole through the center were compressively loaded at the  $6.5 \times 7.5 \text{ mm}^2$  faces within environment-controlled test chamber, which is quartz tube surrounded by high temperature heating tape and fiber insulation. The load was measured using a calibrated load cell (0–9000 N), and the position of planar cracks propagating from the top and bottom of the hole in the glass was monitored as a function of time using a CCD camera and imaging software. Images of a propagating crack plane at various times are shown in Fig. 1(B). The crack velocity was calculated by a simple finite difference between successive data points, i.e.  $v = \Delta L / \Delta t$  where  $\Delta L$  is the incremental crack length and  $\Delta t$  is the incremental time. In the current test geometry, the stress intensity ( $K_I$ ) decreases as crack length increases; hence the velocity decreases with time.  $K_I$  values were calculated from the applied stress, measured crack length, and hole radius using a relationship determined by Michalske et al. [8].

SCG measurements were carried out in an  $\text{N}_2$  atmosphere at different temperatures ( $T$ , 25–450 °C) and water vapor pressures ( $P_{\text{H}_2\text{O}}$ , 0.3–10000 Pa). The water vapor pressure in the test chamber was controlled by the flow of  $\text{N}_2$  gas (from cryogenic supply) that had been bubbled through water in a temperature-controlled water bath. The gas flow rate (5 standard liters/min) was regulated by a mass flow controller (Brooks 5850i), and the input gas supply was preheated to prevent water condensation in the gas lines and to shorten temperature equilibration times in the test chamber. For generating low water vapor pressures (0.3–120 Pa), gas traveling through the water bath was mixed with a controlled amount of dry  $\text{N}_2$  gas. The water vapor pressure was measured from the gas exiting the test chamber using an optical dew point sensor.

The error in the crack velocity was dominated by the error in the measurement of the crack length ( $\pm 10 \text{ }\mu\text{m}$ ) in the CCD camera image. Using standard error propagation calculations, the error in the crack velocity ranged from  $\pm 3\%$  in region III where  $\Delta L$  is relatively large ( $\sim 400 \text{ }\mu\text{m}$ ) to  $\pm 10\%$  in region I where  $\Delta L$  is relatively small ( $\sim 100 \text{ }\mu\text{m}$ ).

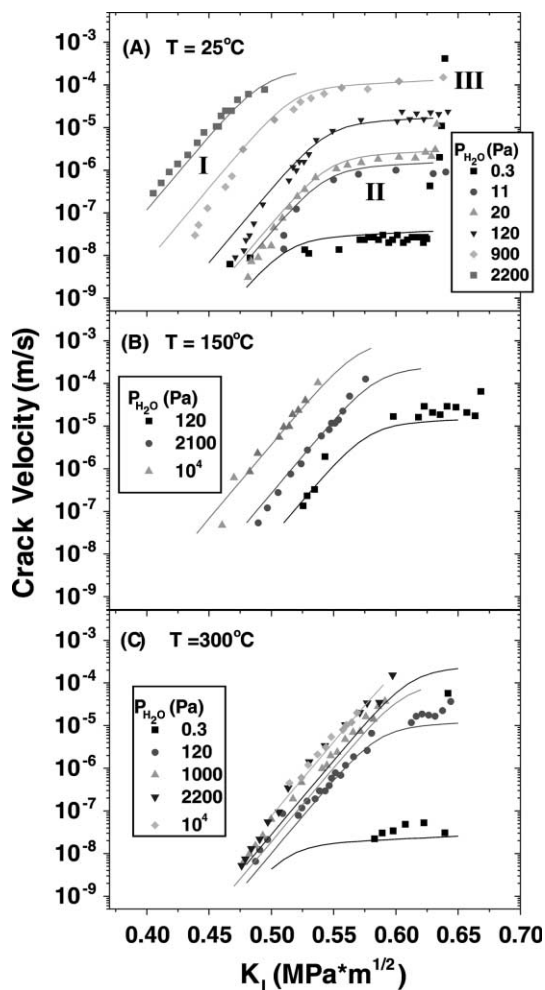


Fig. 2. Crack growth velocities of fused silica glass at (A) 25 °C (B) 150 °C and (C) 300 °C at various  $P_{\text{H}_2\text{O}}$  ranging from 0.3 to 10000 Pa. The points are measured data and the lines represent predicted crack velocities using Eqs. (2), (6) and (9). Each set of points represents data collected from a single sample.

In Figs. 2 and 3, the error bars are no larger than the two times the size of the data points.

### 3. Results

Crack velocity data for oxide glasses are typically plotted as log velocity ( $\log v$ ) vs. stress intensity ( $K_I$ ). Stress intensity is a quantity that describes the driving force for fracture at the crack tip. These data commonly show three distinct

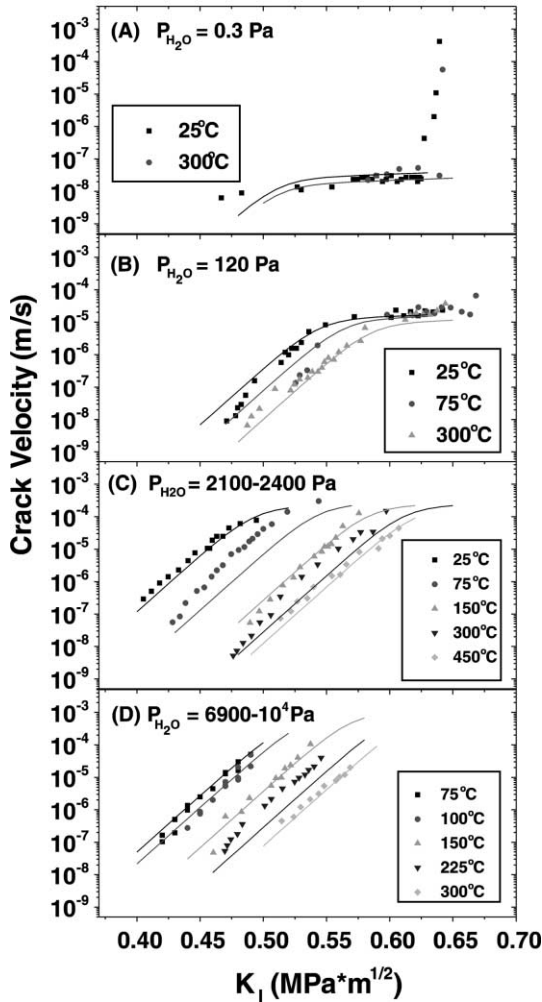


Fig. 3. Crack growth velocities of fused silica glass at  $P_{H_2O}$  of (A) 0.3 Pa, (B) 120 Pa, (C) 2130–2400 Pa and (D) 6900–10 000 Pa at various temperatures ranging from 25 to 450 °C. The points are measured data and the lines represent predicted crack velocities using Eqs. (2), (6) and (9).

regions, designated by regions I, II, and III (see Fig. 2(A)), which can be described in terms of the Si–O–Si bond breakage by a stress–corrosion mechanism [3,11]. Region I refers to the condition when crack growth is reaction-rate limited, and is generally characterized by a near exponential dependence of crack velocity on  $K_I$ . In this region, transport of  $H_2O$  to the crack tip is rapid enough that crack growth is limited only by the rate of reaction between  $H_2O$  and the Si–O–Si bond. In

region II, the crack velocity is no longer reaction-rate-limited, but instead is limited by mass transport (i.e. diffusion) of  $H_2O$  to the crack tip [3]. Consequently, the onset of region II behavior is usually observed at higher stress intensities where crack velocity outpaces the rate at which  $H_2O$  can be supplied to the crack front. Lower water vapor pressures and temperatures generally enhance the onset of region II behavior. The measured crack velocities in region II remain nearly constant with increasing  $K_I$ . Finally, in region III, the crack velocity is no longer limited by mass transport [3]. The onset of region III is indicated by a rapid increase in crack velocity at the end of region II (see Fig. 2(A)). This typically occurs as  $K_I$  approaches the glass fracture toughness; at the fracture toughness limit (i.e.  $K_I = K_{Ic}$ ) the growth velocity approaches a value about 1/3–1/2 of sound speed in the material [12].

The measured slow crack velocities for fused silica at various temperatures and water vapor pressures are shown in Figs. 2 and 3. Figs. 2(A)–(C) are plots at constant temperatures (25, 150, and 300 °C, respectively) illustrating the effect of humidity on the crack velocity. Figs. 3(A)–(D) are plots at constant water vapor pressures (0.3, 120, ~2200, and ~8400 Pa, respectively) illustrating the effect of temperature on the crack velocity. At a fixed  $K_I$ , the crack velocity in fused silica glass increases with humidity in regions I and II. However, the crack velocity decreases with increase in temperature in region I and does not change with temperature in region II.

#### 4. Discussion

##### 4.1. Region I behavior

Hillig and Charles [13] and later Wiederhorn [3,11] have described the region I crack velocities ( $v_I$ ) in glass due to stress corrosion by the following reaction-rate expression:

$$v_I = S \left( \frac{P_{H_2O}}{P_0} \right)^m \exp \left( \frac{K_I b - Q_I}{RT} \right), \quad (1)$$

where  $S$  is a pre-exponential constant (m/s),  $P_{H_2O}$  is the water vapor pressure (Pa),  $P_0$  the atmospheric

pressure ( $10^5$  Pa),  $b$  is a parameter ( $\text{m}^{5/2}/\text{mole}$ ) related to activation volume and radius of curvature of crack tip,  $Q_1$  is the activation energy (kJ/mole), and  $m$  is the ‘order’ of the reaction that often appears in reaction-rate expressions. The above relation predicts an exponential increase in crack velocity with  $K_I$  and an Arrhenius-like increase with temperature. The Arrhenius temperature dependence of SCG (which we call a normal temperature dependence) has been reported in many silicate glasses and non-silicate glasses [9,10,14–16].

The region I temperature dependence for crack growth in fused silica observed in this study is opposite of that found in other glasses (Fig. 4). For example, at a constant water vapor pressure ( $P_{\text{H}_2\text{O}} = 2100\text{--}2400$  Pa) and constant stress intensity (say  $0.49$  MPa $\text{m}^{1/2}$ ), an increase in temperature from 25 to 300 °C produces a  $10^4$  decrease in crack velocity (see Fig. 3(C)). In contrast, the crack velocity of soda-lime silica and phosphate glasses increases by  $10^4$  over the same temperature range [4,10]. The decrease in crack velocities with temperature in fused silica was observed for all

water vapor pressures used in this study (see Fig. 3).

Despite the fact that the temperature dependence of SCG in fused silica glass does not follow the temperature dependence expected with the stress–corrosion mechanism (Eq. (1)), water vapor still enhances crack propagation in a similar manner to that observed in other glasses. Crack velocities have been reported to depend on  $P_{\text{H}_2\text{O}}$  as given by Eq. (1) where  $m$  varies from 0.5 to 2 in fused silica and other glasses [4,10,17]. It is likely that the stress–corrosion mechanism for crack propagation in fused silica still applies; however, some other phenomenon is providing a strong negative temperature dependence that is competing with Arrhenius-type temperature dependence given in Eq. (1).

Anomalous fracture behavior in fused silica was first observed by Wiederhorn et al. [4]. They observed that fused silica glass would not exhibit SCG under vacuum while other glasses did. One explanation given is that high negative pressures (tensile stress) at the crack tip result in a stiffer crack tip [4]. Hence the glass appears more resistant to fracture. Later Fisk and Michalske [18] observed a negative temperature dependence in fused silica SCG at temperatures between 25 and 100 °C at a single water vapor pressure. They proposed this was caused by a decrease in the  $\text{H}_2\text{O}$  activity at the crack tip with temperature, stemming from enhanced adsorbed- $\text{H}_2\text{O}$  desorption rates from the crack tip surface.

To our knowledge, fused silica is the only glass that has been observed to have this anomalous temperature dependence. The structure of silica glass can be described as a random network of interconnected  $\text{SiO}_4$  tetrahedra. These tetrahedra form silica rings, typically consisting of 5–6 Si atoms. Other silicate glasses deviate from this basic structure through the addition of alkali metal and alkaline earth oxides that act as network modifiers [19]. In addition to other glasses, quartz (a crystalline form of  $\text{SiO}_2$ ) also shows normal temperature dependence of SCG [20]. Hence, we speculate that the mechanism for this anomalous behavior stems from structure (not just the glass composition) of the silica glass. Also, the anomalous behavior is likely not a result of a unique surface

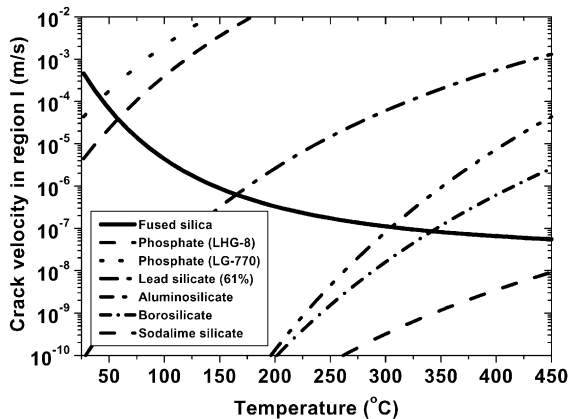


Fig. 4. Comparison of SCG velocities in region I of different glasses as a function of temperature. The lines represent model fits to the data. All velocities were determined at stress intensities that are 80% of the fracture toughness of that glass. Dashed lines are from data on various silicate glasses measured in vacuum [4,32] and on various phosphate glasses measured in an  $\text{N}_2$  atmosphere at  $P_{\text{H}_2\text{O}} = 2700$  Pa [9,10]. The solid line is from data on fused silica measured in  $\text{N}_2$  atmosphere at  $P_{\text{H}_2\text{O}} = 2700$  Pa from this study.

chemistry of SiO<sub>2</sub>, since both fused silica and quartz should have similar surface chemistries.

The word ‘anomalous’ has been used to describe many of the properties of fused silica [21–23]. For example, the thermal expansion coefficient, specific heat, compressibility, elastic modulus, acoustic loss and dielectric loss are all considered anomalous in fused silica [21–23]. Consider the elastic modulus; it increases with both temperature and applied tensile stress. In other words, temperature and tensile stress stiffen the glass [24–26]. Most glasses exhibit the opposite trend. Some have suggested that these anomalous properties stem from a change in Si–O–Si bond angle with change in temperature and pressure [21,27]. Although lacking direct evidence of structural rearrangement, indirect structural measurements and molecular modeling show that such a rearrangement of the SiO<sub>4</sub> tetrahedra can occur [21,27,28].

We speculate that the same proposed structural change in the silica glass structure that has been used to explain the other anomalous properties of fused silica may also explain the negative temperature dependence of SCG in vitreous silica. Spe-

cifically, a change in the distribution of oxygen bond angles in the vitreous network can modify the material properties such that the crack tip stiffens under tensile stress and at higher temperatures [21,27,28]. Another possibility is the structural change with temperature results in a weaker temperature dependence (i.e. lower activation energy) for the stress corrosion reaction causing H<sub>2</sub>O desorption rates at the crack surface to dominate [18]. However, regardless of the mechanism, the SCG behavior in region I for fused silica over most of the temperatures and water vapor pressures examined in this study can be described using an empirical relationship, such as

$$v_I = \exp \left[ -A + BK_I \frac{CP_{H_2O}^{1/3}}{T^3} \right], \quad (2)$$

where *A*, *B*, *C* are constants with best-fit values of 59, 80 MPa m<sup>1/2-1</sup>, and 2.3 × 10<sup>7</sup> K<sup>3</sup>/Pa<sup>1/3</sup>, respectively, determined by multiple non-linear regression analysis. The empirical relationship does a reasonable job describing measured crack velocities in region I (Figs. 2 and 3).

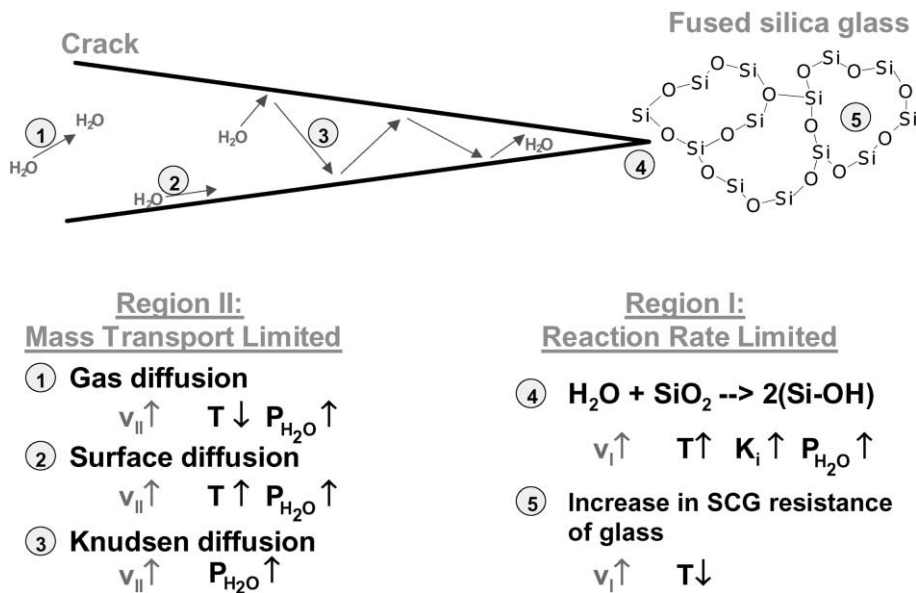


Fig. 5. Schematic illustrating the types of processes governing mass transport of H<sub>2</sub>O and the possible interactions governing crack propagation. The up/down arrows in the bottom half of the figure describe the increase/decrease of the term listed to the left. For example, crack velocity in region II (*v*<sub>II</sub>) will increase with increase in water vapor pressure (*P*<sub>H<sub>2</sub>O</sub>) and will increase with decrease in temperature for process 1, gas diffusion.

#### 4.2. Region II behavior

In region II, the rate of mass transport of H<sub>2</sub>O to the crack tip limits the rate of crack propagation. Mass transport to the crack tip is controlled by H<sub>2</sub>O diffusion through the crack either by gas, along the fracture surface, or by Knudsen diffusion (see Fig. 5). The crack velocity in region II for fused silica increases linearly with water vapor pressure, and is essentially independent of temperature and stress intensity (see Figs. 2 and 3).

For other glasses previously examined (e.g., metaphosphate glasses), crack velocity in region II show an Arrhenius-type temperature dependence [9,10]. Mass transport is controlled by surface diffusion of H<sub>2</sub>O to the crack tip in these glasses [9,10]. When measured at the same temperature and humidity, phosphate glass SCG in region II is about 100× slower than in fused silica (Fig. 6). This suggests that the mechanism of H<sub>2</sub>O transport to the crack tip is different in these glasses. Also, because the region II crack velocity in fused silica was essentially independent of temperature, it cannot be explained by surface diffusion (Fig. 5).

However, mass transport by Knudsen diffusion does coincide with the observed temperature behavior for fused silica. A Knudsen diffusion mass-transport model to describe SCG was originally developed by Lawn [12,29,30]. In the model, H<sub>2</sub>O vapor transports to the crack tip by free molecular

flow (gas diffusion) as long as the crack width is larger than the mean free path of H<sub>2</sub>O. However, as the crack width gets narrower near the crack tip, H<sub>2</sub>O vapor transport becomes impeded by the collisions with the wall of the crack. Knudsen showed for that gas flow through a narrow pore impedes vapor transport [31].

In Lawn's model [28], the crack velocity in region II ( $v_{II}$ ), the Knudsen impedance factor ( $\kappa$ ), and the mean free path ( $\lambda$ ) are given by

$$v_{II} = \frac{\kappa(P_{H_2O} - P_c)A_1}{\eta N_A (2\pi m_{H_2O} kT)^{1/2}}, \quad (3)$$

$$\kappa = \frac{32K_i^2}{3\pi E^2 a_0 \ln(\lambda/a_0)} \quad (4)$$

and

$$\lambda = \frac{kT}{\sqrt{2}\pi\sigma^2 P_0}, \quad (5)$$

where  $\eta$  is the reaction order,  $N_A$  is number of bonds intersecting area of crack plane (#/m<sup>2</sup>),  $A_1$  is the width of crack tip (m),  $m_{H_2O}$  is molecular weight of H<sub>2</sub>O (g/mol),  $k$  is Boltzmann's constant, the  $a_0$  is adsorption site spacing (m),  $\lambda$  is the mean free path of H<sub>2</sub>O (m),  $\sigma$  is the cross-section of the gas species (m<sup>2</sup>),  $P_c$  is the minimum H<sub>2</sub>O pressure required for crack propagation (Pa), and  $E$  is Young's modulus for fused silica (Pa).

Substituting Eqs. (4) and (5) into Eq. (3), and assuming  $P_c = 0$  the crack velocity in region II simplifies to the following relation:

$$v_{II} = F \frac{K_i^2 P_{H_2O}}{\ln(GT)T^{1/2}}, \quad (6)$$

where  $F$  and  $G$  are

$$F = \frac{32A_1}{3\pi a_0 E^2 N_A \eta (2\pi m_{H_2O} k)^{1/2}} \quad (7)$$

and

$$G = \frac{k}{\sqrt{2}\pi P_0 \sigma^2 a_0}. \quad (8)$$

During the SCG measurements, the atmosphere contains H<sub>2</sub>O and N<sub>2</sub>. We used the cross-section ( $\sigma$ ) of N<sub>2</sub> (3.75 Å) to calculate the mean free path (see [12,28,29]), because the majority of the gas is

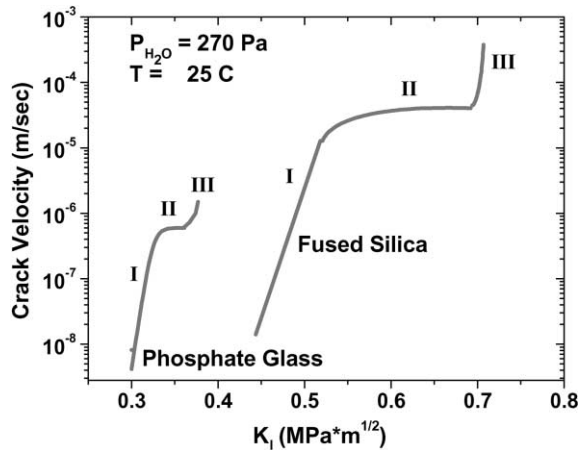


Fig. 6. Comparison of SCG velocities for fused silica and a metaphosphate glass measured at 298 K and 270 Pa P<sub>H<sub>2</sub>O</sub>.

$N_2$  and hence the majority of molecular collisions are due to  $N_2$ , not  $H_2O$ . The mean free path ranges from 60 to 150 nm. The order of the reaction ( $\eta$ ) is assumed to be 1. Also, we used  $E = 73$  GPa,  $m_{H_2O} = 18$  g/mol,  $a_0 = 3.2$  Å (Si–O–Si bond length),  $N_A = 9.8 \times 10^{18}$  m $^{-2}$  (based on a Si–O–Si bond length of 3.2 Å),  $A_1 = 3.2$  Å, and  $P_0 = 1$  atm. The values of  $F$  and  $G$  for fused silica are then determined as  $4 \times 10^{-17}$  K $^{1/2}$ /(Pa $^3$  s) and  $0.681$  K $^{-1}$ .

Notice that Eq. (6) predicts a linear increase in the crack velocity with water vapor pressure. Although there is a temperature and stress intensity dependence in Eq. (6), they are both relatively weak. In the work reported here, the temperature and stress intensity vary by a factor of 2, whereas the  $P_{H_2O}$  varies by  $10^4$ . The region II crack velocity described by Eq. (6) are compared to the experimental data taken on fused silica in Fig. 7. Calculations of the crack velocity were performed at two temperatures, 300 and 700 K. Notice the relatively weak temperature dependence of the model and the data. The measured region II crack velocities are well described by the Knudsen diffusion model as shown in Fig. 7.

The expressions for  $v_I$  and  $v_{II}$  (i.e., Eqs. (2) and (6)) describe the crack growth velocity in the limits

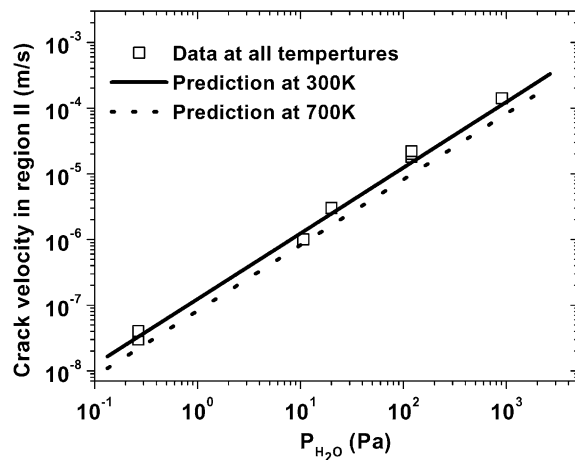


Fig. 7. Crack growth velocity ( $v_{II}$ ) of fused silica glass in region II as a function of water vapor pressure in the environment. The points represent measured velocities and the lines represent model predictions using Eq. (6). Note that the measured data is shown for data at temperatures ranging from 25 to 300 °C.

of region I and II, respectively. These two velocities can be combined into a single expression describing the composite SCG velocity across both regions I and II:

$$v = \frac{v_I v_{II}}{v_I + v_{II}}, \quad (9)$$

where the composite crack growth velocity ( $v$ ) is the harmonic mean of the crack velocity,  $v_I$ , in region I (Eq. (2)) and,  $v_{II}$ , in region II (Eq. (3)) [29]. Note that in the limit of region I, Eq. (9) approaches  $v \rightarrow v_I$ , and similarly in region II,  $v \rightarrow v_{II}$ . The velocities calculated by Eq. (9) are compared to the experimental data in Figs. 2 and 3. Using a single set of parameters, these expressions do a reasonable job predicting measured crack velocities at various temperatures and water vapor pressures. These expressions for crack velocities in fused silica should serve as a useful tool to predict crack velocities and hence lifetimes of glass parts exposed to various temperatures, water vapor pressures, and stresses.

## 5. Conclusions

In contrast to other inorganic glasses measured to date, the temperature dependence of SCG in fused silica is anomalous. In region I, crack velocities of fused silica were found to decrease with increase in temperature at a constant water vapor pressure. This negative temperature dependence is believed to stem from a change in the slow crack growth resistance of the glass upon exposure to temperature and stress, a process that competes with the expected normal temperature dependence as predicted by the stress–corrosion mechanism. An empirical relationship does a reasonable job at describing the crack velocities in region I at various temperatures, water vapor pressures and stress. In region II, crack velocities were found to be independent of temperature. In contrast, other glasses (such as metaphosphates) were shown to have crack velocities that increase with temperature in region II. A mass-transport model based on Knudsen diffusion developed by Lawn can quantitatively described the measured crack velocities in region II.

## Acknowledgements

This work was performed under the auspices of the US Department of Energy by the University of California, Lawrence Livermore National Laboratory under contract no. W-7405-Eng-48 in the Laboratory Directed Research and Development (LDRD) Program.

## References

- [1] T. Michalske, B. Bunker, *Sci. Am.* 257 (1987) 78.
- [2] T.A. Michalske, S.W. Freiman, *J. Am. Ceram. Soc.* 66 (1983) 284.
- [3] S. Wiederhorn, *J. Am. Ceram. Soc.* 55 (1972) 81.
- [4] S. Wiederhorn, H. Johnson, A. Diness, A. Heuer, *J. Am. Ceram. Soc.* 57 (1974) 336.
- [5] J. West, L. Hench, *Philos. Mag.* 77 (1998) 85.
- [6] Y. Hibino, S. Sakaguchi, Y. Tajima, *J. Am. Ceram. Soc.* 67 (1984) 64.
- [7] M. Muraoka, H. Abe, *J. Am. Ceram. Soc.* 79 (1996) 51.
- [8] T. Michalske, W. Smith, E. Chen, *Eng. Fract. Mech.* 45 (1993) 637.
- [9] T.I. Suratwala, R.A. Steele, G.D. Wilke, J.H. Campbell, K. Takeuchi, *J. Non-Cryst. Solids* 263&264 (2000) 213.
- [10] S. Crichton, M. Tomozawa, J. Hayden, T. Suratwala, J. Campbell, *J. Am. Ceram. Soc.* 82 (1999) 3097.
- [11] S. Wiederhorn, in: R. Brandt, D. Hasselman, F. Lange (Eds.), *Fracture Mechanics in Ceramics*, Plenum, New York, 1978, p. 549.
- [12] B. Lawn, *Fracture of Brittle Solids*, 2nd Ed., Cambridge University, Cambridge, 1993.
- [13] W. Hillig, R. Charles, in: V. Zacklay (Ed.), *High Strength Materials*, John Wiley, New York, 1965, p. 682.
- [14] S. Wiederhorn, *J. Am. Ceram. Soc.* 50 (1967) 407.
- [15] S. Wiederhorn, in: R. Bradt, D. Hasselman, F. Lange (Eds.), *Fracture Mechanics of Ceramics*, Plenum, New York, 1996, p. 613.
- [16] T. Michalske, B. Bunker, *J. Am. Ceram. Soc.* 76 (1993) 2613.
- [17] S. Wiederhorn, E.R. Fuller Jr., R. Thomson, *Met. Sci.* 450 (1980).
- [18] G.A. Fisk, T.A. Michalske, *J. Appl. Phys.* 58 (1985) 2736.
- [19] B. Atkinson, *J. Geophys. Res.* 89 (1984) 4077.
- [20] W.D. Kingery, H.K. Bowen, D.R. Uhlmann, *Introduction to Ceramics*, 2nd Ed., John Wiley, New York, 1976.
- [21] M. Vucevich, *J. Non-Cryst. Solids* 11 (1972) 25.
- [22] R. Bruckner, *J. Non-Cryst. Solids* 5 (1970) 123.
- [23] V. Shutilov, B. Abezgauz, *Sov. J. Glass Phys. Chem.* 11 (1982) 129.
- [24] F. Mallinder, B. Proctor, *Phys. Chem. Glasses* 5 (1964) 91.
- [25] S. Spinner, *J. Am. Ceram. Soc.* 39 (1956) 113.
- [26] D. Tallant, T. Michalske, W. Smith, *J. Non-Cryst. Solids* 106 (1988) 380.
- [27] C. Angell, J. Shao, M. Grabow, *Proceeding of the Workshop of Non-equilibrium Phenomena in Supercooled Fluids, Glasses and Amorphous Materials*, vol. 50, 1996.
- [28] K. Trachenko, M. Dove, M. Harris, V. Heine, *J. Phys.: Condens. Matter* 12 (2000) 8041.
- [29] B. Lawn, *Mater. Sci. Eng.* 13 (1974) 277.
- [30] B. Lawn, *J. Mater. Sci.* 10 (1975) 469.
- [31] M. Knudsen, *The Kinetic Theory of Gases*, Methuen, London, 1950.
- [32] S.M. Wiederhorn, *J. Am. Ceram. Soc.* 52 (1969) 99.